

Two-dimensional ring-like vortex and multisoliton nonlinear structures at the upper-hybrid resonance

V. M. Lashkin*

Institute for Nuclear Research, Pr. Nauki 47, Kiev 03680, Ukraine

(Dated: February 1, 2008)

Two-dimensional (2D) equations describing the nonlinear interaction between upper-hybrid and dispersive magnetosonic waves are presented. Nonlocal nonlinearity in the equations results in the possibility of existence of stable 2D nonlinear structures. A rigorous proof of the absence of collapse in the model is given. We have found numerically different types of nonlinear localized structures such as fundamental solitons, radially symmetric vortices, nonrotating multisolitons (two-hump solitons, dipoles and quadrupoles), and rotating multisolitons (azimuthons). By direct numerical simulations we show that 2D fundamental solitons with negative hamiltonian are stable.

PACS numbers:

I. INTRODUCTION

Upper-hybrid (UH) waves are frequently observed in space and laboratory plasmas. The UH waves can be excited by beam instabilities, mode conversion of extraordinary electromagnetic waves at the upper-hybrid resonance layer, etc.¹ One-dimensional (1D) theory of the nonlinear UH waves interacting with the low-frequency motions of magnetosonic type was developed in Refs. 2–7. In particular, for low frequency magnetohydrodynamic perturbations with frozen-in field lines and for the negative group dispersive UH waves, Kaufman and Stenflo² showed the existence of UH solitons with compressional density (magnetic field) perturbations in the super-magnetosonic regime. Dispersive magnetosonic/lower-hybrid waves interacting with high-frequency one-dimensional UH waves were first considered in Refs. 4 and 5 and then were studied in more detail, including intensive numerical modelling⁷.

The aim of this paper is to present two-dimensional (2D) theory of nonlinearly coupled dispersive magnetosonic and high-frequency UH waves. We have derived a set of corresponding nonlinear equations and found numerically different types of 2D nonlinear localized structures such as fundamental solitons, radially symmetric vortices, nonrotating multisolitons (dipoles and quadrupoles), and rotating multisolitons (azimuthons).

Dispersion of the magnetosonic wave effectively introduces a nonlocal nonlinear interaction, that is the nonlinear response depends on the wave packet intensity at some extensive spatial domain. Nonlocal nonlinearity naturally arises in many areas of nonlinear physics and plays a crucial role in the dynamics of nonlinear coherent structures. While collapse is a usual phenomenon in the multidimensional Zakharov-like models with local low-frequency response, nonlocal nonlinearity can arrest collapse and lead to stable multidimensional localized structures^{8,9,10,11,12,13}. Turitsyn proved¹⁴ the absence of collapse for three particular shapes of the nonlocal nonlinear response in the multidimensional generalized nonlinear Schrödinger equation (GNSE). Later, a rigorous proof of absence of collapse in arbitrary spa-

tial dimensions during the wave-packet propagation described by the nonlocal GNSE with sufficiently general symmetric response kernel was presented in Ref. 15. In the present paper we give a proof of absence of collapse for the 2D model describing the nonlinear interaction between upper-hybrid and dispersive magnetosonic waves.

The paper is organized as follows. In Sec. II, we present the generalized Zakharov-type system of 2D equations, describing the interaction between high-frequency upper-hybrid waves and low-frequency dispersive magnetosonic waves. A linear stability analysis is performed in Sec. III. Section IV contains the rigorous proof of absence of collapse in the model. Localized nonlinear solutions, including vortex ring-like, nonrotating (a monopole, a dipole, and a quadrupole) and rotating (azimuthons) multisoliton solutions are presented in Sec. V. The conclusion is made in Sec. VI.

II. DERIVATION OF EQUATIONS

We consider a homogeneous electron-ion plasma in a uniform external magnetic field $\mathbf{B}_0 = B_0 \hat{\mathbf{z}}$, where $\hat{\mathbf{z}}$ is the unit vector along the z direction. In the linear approximation, the UH waves are characterized by the dispersion relation

$$\omega = \omega_{UH} \left(1 + \frac{1}{2} k_{\perp}^2 R^2 \alpha \right), \quad (1)$$

where $\omega_{UH} = (\omega_{pe}^2 + \omega_{ce}^2)^{1/2}$ is the UH resonance frequency, ω_{pe} (ω_{ce}) is the electron plasma (gyro) frequency, $v_{te} = (T_e/m)^{1/2}$ is the electron thermal speed, $\alpha = \omega_{pe}^2 / (\omega_{pe}^2 - 3\omega_{ce}^2)$, and $R^2 = 3v_{te}^2 / \omega_{UH}^2$. Note that the dispersion of the UH waves is negative for $\omega_{pe}^2 < 3\omega_{ce}^2$.

Equation for the slow varying complex amplitude φ of the potential of the high-frequency electrostatic electric field

$$\mathbf{E}^H = -\frac{1}{2} [\nabla \varphi \exp(-i\omega_{UH}t) + \text{c.c.}] \quad (2)$$

of the upper hybrid wave can be obtained from the equa-

tion

$$\nabla \cdot (\hat{\varepsilon} \nabla \varphi) = 0. \quad (3)$$

with

$$\hat{\varepsilon} = \begin{pmatrix} \varepsilon_{\perp} & ig & 0 \\ -ig & \varepsilon_{\perp} & 0 \\ 0 & 0 & \varepsilon_{\parallel} \end{pmatrix}, \quad (4)$$

where the dielectric tensor $\hat{\varepsilon}$ is considered as a differential operator with $\omega \rightarrow \omega_{UH} + i\partial/\partial t$ (assuming $\omega_{UH} \gg \partial/\partial t$) and $\mathbf{k} \rightarrow -i\nabla$. Under this, the nonlinear perturbations of the plasma density δn and magnetic field δB are taken into account in ε_{\perp} , ε_{\parallel} and g , so that substitutions $n_0 \rightarrow n_0 + \delta n$ and $B_0 \rightarrow B_0 + \delta B$ are made in the resulting equation

$$\nabla_{\perp} \cdot (\varepsilon_{\perp} \nabla_{\perp} \varphi) + \frac{\partial}{\partial z} \left(\varepsilon_{\parallel} \frac{\partial \varphi}{\partial z} \right) + i\hat{\mathbf{z}} \times \nabla g \cdot \nabla \varphi = 0. \quad (5)$$

As a result, we have

$$\begin{aligned} & \Delta \left(2i\omega_{UH} \frac{\partial \varphi}{\partial t} + 3v_{te}^2 \alpha \Delta \varphi \right) + \frac{\omega_{pe}^2 \omega_{ce}^2}{\omega_{UH}^2} \frac{\partial^2 \varphi}{\partial z^2} \\ & = \nabla \cdot \left\{ \left(\omega_{pe}^2 \frac{\delta n}{n_0} + 2\omega_{ce}^2 \frac{\delta B}{B_0} \right) \nabla \varphi \right. \\ & \quad \left. - i \frac{\omega_{ce}}{\omega_{UH}} \left[\omega_{pe}^2 \frac{\delta n}{n_0} + (\omega_{pe}^2 + 2\omega_{ce}^2) \frac{\delta B}{B_0} \right] \nabla \varphi \times \hat{\mathbf{z}} \right\}. \end{aligned} \quad (6)$$

The second term in the $\{\dots\}$ bracket in Eq. (6) comes from the last term in Eq. (5) and corresponds to the so-called vector nonlinearity. This term is identically zero for 1D case and for the fields with axial symmetry. This term can also be neglected if $\omega_{ce}/\omega_{pe} \ll 1$.

The upper-hybrid waves have wave numbers almost normal to the external magnetic field ($k_z \ll k_{\perp}$) and, in the following, we will consider two-dimensional (2D) case with $k_z = 0$ so that $\Delta = \partial^2/\partial x^2 + \partial^2/\partial y^2$ and $\nabla = (\partial/\partial x, \partial/\partial y)$.

The low-frequency motion of the plasma is governed by the continuity and momentum equations for ions and electrons. We assume quasineutrality condition, so that $\delta n_i = \delta n_e \equiv \delta n$. Thus, we have

$$\frac{\partial \delta n}{\partial t} + n_0 \nabla \cdot \mathbf{v}_i = 0, \quad (7)$$

$$\frac{\partial \mathbf{v}_i}{\partial t} = \frac{e}{M} \mathbf{E} - \frac{\gamma_i T_i}{n_0 M} \nabla \delta n + \omega_{ci} [\mathbf{v}_i \times \hat{\mathbf{z}}], \quad (8)$$

$$\frac{\partial \delta n}{\partial t} + n_0 \nabla \cdot \mathbf{v}_e + \nabla \cdot \mathbf{F}_2 = 0, \quad (9)$$

$$\frac{\partial \mathbf{v}_e}{\partial t} + \mathbf{F}_1 = -\frac{e}{m} \mathbf{E} - \frac{\gamma_e T_e}{n_0 m} \nabla \delta n - \omega_{ce} [\mathbf{v}_e \times \hat{\mathbf{z}}], \quad (10)$$

where γ_i (γ_e) is the ion (electron) ratio of specific heats, and

$$\mathbf{F}_1 = \langle (\mathbf{v}^H \cdot \nabla) \mathbf{v}^H \rangle + \left\langle \frac{e}{mc} [\mathbf{v}^H \times \mathbf{B}^H] \right\rangle, \quad \mathbf{F}_2 = \langle n^H \mathbf{v}^H \rangle \quad (11)$$

are nonlinear terms in electron equations, the angular brackets denote averaging over the high-frequency oscillations, and the superscripts H denote corresponding quantities for the high-frequency fields. Multiplying Eq. (10) by m/M and adding with Eq. (8), we have

$$\frac{\partial}{\partial t} \left(\mathbf{v}_i + \frac{m}{M} \mathbf{v}_e \right) = -\frac{m}{M} \mathbf{F}_1 - \frac{v_s^2}{n_0} \nabla \delta n - \omega_{ci} [(\mathbf{v}_e - \mathbf{v}_i) \times \hat{\mathbf{z}}], \quad (12)$$

where we have introduced the effective sound speed $v_s = \sqrt{(\gamma_i T_i + \gamma_e T_e)/M}$. Taking the div from Eq. (12) we get

$$\begin{aligned} & \frac{\partial}{\partial t} \left(\nabla \cdot \mathbf{v}_i + \frac{m}{M} \nabla \cdot \mathbf{v}_e \right) = -\frac{m}{M} \nabla \cdot \mathbf{F}_1 \\ & \quad - \frac{v_s^2}{n_0} \Delta \delta n - \omega_{ci} \hat{\mathbf{z}} \cdot \nabla \times (\mathbf{v}_e - \mathbf{v}_i). \end{aligned} \quad (13)$$

Using Eqs. (7) and (9), and eliminating $\nabla \times (\mathbf{v}_e - \mathbf{v}_i)$ with the aid of the Maxwell equation (we neglect the displacement current for the low-frequency motion)

$$\nabla \times \delta \mathbf{B} = \frac{4\pi e n_0}{c} (\mathbf{v}_i - \mathbf{v}_e), \quad (14)$$

one can obtain

$$\begin{aligned} & \frac{\partial^2 \delta n}{\partial t^2} - v_s^2 \Delta \delta n - \frac{n_0}{B_0} v_A^2 \Delta \delta B = \frac{m n_0}{M} \nabla \cdot \mathbf{F}_1 \\ & \quad - \frac{m}{M} \nabla \cdot \frac{\partial \mathbf{F}_2}{\partial t}, \end{aligned} \quad (15)$$

where $v_A = B_0/\sqrt{4\pi n_0 M}$ is the Alfvén speed. The second term in the right-hand side of Eq. (15) is small compared to the first one by the factor $\sim \omega/\omega_{UH}$ and can be neglected. To obtain equation for the low-frequency magnetic field perturbation δB we subtract Eq. (10) from Eq. (8) and take the curl

$$\begin{aligned} & \frac{\partial}{\partial t} \nabla \times (\mathbf{v}_i - \mathbf{v}_e) = \frac{e}{m} \nabla \times \mathbf{E} - \omega_{ci} \hat{\mathbf{z}} \nabla \cdot \mathbf{v}_i \\ & \quad - \omega_{ce} \hat{\mathbf{z}} \nabla \cdot \mathbf{v}_e + \nabla \times \mathbf{F}_1. \end{aligned} \quad (16)$$

Using Eqs. (7), (9), (14) and the Maxwell equation

$$\nabla \times \mathbf{E} = -\frac{1}{c} \frac{\partial \delta \mathbf{B}}{\partial t} \quad (17)$$

we get

$$\frac{\partial}{\partial t} \left(1 - \frac{c^2}{\omega_{pe}^2} \Delta \right) \delta B - \frac{B_0}{n_0} \frac{\partial \delta n}{\partial t} = \frac{4\pi c}{\omega_{pe}^2} (\nabla \times \mathbf{F}_1)_z. \quad (18)$$

Representing

$$\mathbf{v}_e^H = \frac{1}{2} [\mathbf{v} \exp(-i\omega_{UH} t) + \text{c.c.}], \quad (19)$$

from the high-frequency momentum equation for electrons we have

$$\mathbf{v} = \frac{e}{m} \frac{[i\omega_{UH} \nabla \varphi + \omega_{ce}(\nabla \varphi \times \hat{\mathbf{z}})]}{(\omega_{UH}^2 - \omega_{ce}^2)}. \quad (20)$$

With the aid of the Maxwell equation for $\partial \mathbf{B}^H / \partial t$, two terms in the expression for \mathbf{F}_1 can be combined to yield

$$\begin{aligned} \mathbf{F}_1 &= \langle (\mathbf{v}_e^H \cdot \nabla) \cdot \mathbf{v}_e^H + [\mathbf{v}_e^H \times [\nabla \times \mathbf{v}_e^H]] \rangle \\ &= \frac{1}{2} \langle \nabla (\mathbf{v}_e^H \cdot \mathbf{v}_e^H) \rangle. \end{aligned} \quad (21)$$

Using Eqs. (15), (18)–(21) we obtain equations for the low-frequency plasma density and magnetic field perturbations

$$\begin{aligned} \left(\frac{\partial^2}{\partial t^2} - v_s^2 \Delta \right) \frac{\delta n}{n_0} - v_A^2 \Delta \frac{\delta B}{B_0} &= \frac{1}{16\pi n_0 M} \\ &\times \Delta \left\{ \left(1 + 2 \frac{\omega_{ce}^2}{\omega_{pe}^2} \right) |\nabla \varphi|^2 \right. \\ &\left. + 2i \left(1 + \frac{\omega_{ce}^2}{\omega_{pe}^2} \right) \frac{\omega_{ce}}{\omega_{UH}} [\nabla \varphi \times \nabla \varphi^*]_z \right\}, \end{aligned} \quad (22)$$

$$\left(1 - \frac{c^2}{\omega_{pe}^2} \Delta \right) \frac{\delta B}{B_0} = \frac{\delta n}{n_0}. \quad (23)$$

In the linear approximation, Eqs. (22) and (23) give the dispersion relation for the dispersive fast magnetosonic wave

$$\Omega_k^2 = k_\perp^2 v_s^2 + \frac{k_\perp^2 v_A^2}{1 + k_\perp^2 c^2 / \omega_{pe}^2}. \quad (24)$$

In what follows we omit the subscript \perp in k_\perp . Equations (6), (22) and (23) form a closed system of 2D equations describing the interaction between upper-hybrid waves and dispersive magnetosonic waves. In the 1D case these equations coincide with those obtained in Refs. 4, 5 and 7.

III. NONLINEAR DISPERSION RELATION

In this section we consider the linear theory of the modulational instability of a pump wave with a frequency close to the upper-hybrid frequency. As usual, we express the low-frequency perturbation of the plasma density as

$$\frac{\delta n}{n_0} = \hat{n} \exp(i\mathbf{k} \cdot \mathbf{r} - i\Omega t) + \text{c.c.}, \quad (25)$$

$$\frac{\delta B}{B_0} = \hat{b} \exp(i\mathbf{k} \cdot \mathbf{r} - i\Omega t) + \text{c.c.}, \quad (26)$$

while the upper-hybrid wave is decomposed into the pump wave and two sidebands

$$\begin{aligned} \varphi &= \varphi_0 e^{i(\mathbf{k}_0 \cdot \mathbf{r} - \delta_0 t)} + \varphi_+ e^{i[(\mathbf{k}_0 + \mathbf{k}) \cdot \mathbf{r} - (\delta_0 + \Omega)t]} \\ &+ \varphi_- e^{i[(\mathbf{k}_0 - \mathbf{k}) \cdot \mathbf{r} - (\delta_0 - \Omega)t]} + \text{c.c.}, \end{aligned} \quad (27)$$

where $\delta_0 = \omega_{UH} k_0^2 R^2 / 2$. The amplitudes of the satellites can be calculated from Eq. (6). We have

$$D_+ \varphi_+ = \alpha_+ \hat{n} \varphi_0, \quad (28)$$

$$D_- \varphi_-^* = \alpha_- \hat{n} \varphi_0^*, \quad (29)$$

where

$$\begin{aligned} \alpha_\pm &= -(k_0^2 \pm \mathbf{k} \cdot \mathbf{k}_0) \left(\omega_{pe}^2 + \frac{2\omega_{ce}^2}{1 + k^2 \lambda_e^2} \right) \\ &+ i(\mathbf{k} \times \mathbf{k}_0)_z \frac{\omega_{ce}}{\omega_{UH}} \left(\omega_{pe}^2 + \frac{\omega_{pe}^2 + 2\omega_{ce}^2}{1 + k^2 \lambda_e^2} \right), \end{aligned} \quad (30)$$

and the function

$$D_\pm = 2\omega_{UH}(\mathbf{k}_0 \pm \mathbf{k})^2 (\delta_\pm \mp \Omega) \quad (31)$$

is the Fourier transform of the linear operator in the left-hand side of Eq. (6) evaluated at $\mathbf{k}_0 \pm \mathbf{k}$, and $\delta_\pm = \omega_{UH} R^2 [(\mathbf{k}_0 \pm \mathbf{k})^2 - k_0^2] / 2$ are the mismatches between the satellite frequencies and the frequency of the pump wave. The amplitudes of the low-frequency perturbations are found from Eqs. (22) and (23):

$$(\Omega^2 - \Omega_k^2) \hat{n} = \frac{k^2 (\beta_+ \varphi_+ \varphi_0^* + \beta_- \varphi_-^* \varphi_0)}{16\pi n_0 M}, \quad (32)$$

$$(1 + k^2 c^2 / \omega_{pe}^2) \hat{b} = \hat{n}, \quad (33)$$

where

$$\begin{aligned} \beta_\pm &= \left(1 + 2 \frac{\omega_{ce}^2}{\omega_{pe}^2} \right) (k_0^2 \pm \mathbf{k} \cdot \mathbf{k}_0) \\ &+ 2i \left(1 + \frac{\omega_{ce}^2}{\omega_{pe}^2} \right) (\mathbf{k} \times \mathbf{k}_0)_z \end{aligned} \quad (34)$$

and Ω_k^2 is determined by Eq. (24). By combining Eqs. (28), (29) and (32) one can obtain a nonlinear dispersion relation

$$\Omega^2 - \Omega_k^2 = \frac{k^2 |\varphi_0|^2}{16\pi n_0 M} \left(\frac{\alpha_+ \beta_+}{D_+} + \frac{\alpha_- \beta_-}{D_-} \right). \quad (35)$$

Equation (35) generalizes the nonlinear dispersion relation obtained by Eliasson and Shukla⁷ by considering 2D case and including the vector nonlinearity. For 1D case we recover the previous result. Note, that in the case of coplanar (in the plane perpendicular to the magnetic field) wave vectors $\mathbf{k} \parallel \mathbf{k}_0$, the parametric coupling of the waves due to the vector nonlinearity is absent, while the coupling due to the scalar nonlinearity is the most effective. In the opposite case, i.e. $\mathbf{k} \perp \mathbf{k}_0$, the interaction due to the vector nonlinearity is the most effective, while the interaction due to the scalar nonlinearity is the least effective (and absent for $k_0 \ll k$). In general case $\mathbf{k} \nparallel \mathbf{k}_0$, and when $\omega_{pe} \sim \omega_{ce}$ so that both types of the nonlinearities yield comparable contribution, this leads

to a rather complicated picture of the parametric instability. In this paper, we restrict ourselves to the case of a weakly magnetized plasma with $\omega_{ce}^2/\omega_{pe}^2 \ll 1$. Results, concerning the case of a moderately magnetized plasma with $\omega_{ce} \sim \omega_{pe}$, including the nonlinear analysis (see below), will be published elsewhere.

In the case $\omega_{ce} \ll \omega_{pe}$, one can neglect the vector nonlinearity and Eq. (35) takes the form

$$\Omega_k^2 - \Omega^2 = \frac{|E_0|^2 k^2 \omega_{pe}}{32\pi n_0 M} \left[\frac{\cos^2 \mu_+}{(\delta_+ - \Omega)} + \frac{\cos^2 \mu_-}{(\delta_- + \Omega)} \right], \quad (36)$$

where

$$|E_0|^2 = k_0^2 |\varphi_0|^2, \quad \cos \mu_{\pm} = \frac{\mathbf{k}_0 \cdot (\mathbf{k}_0 \pm \mathbf{k})}{k_0 |\mathbf{k}_0 \pm \mathbf{k}|}. \quad (37)$$

When both sidebands are resonant and the low-frequency perturbations are nonresonant, we can consider the limiting case $\mathbf{k}_0 \gg \mathbf{k}$ and $\Omega_k \gg \Omega$. Then, the dispersion relation Eq. (36) takes the form

$$(\Omega - \mathbf{k} \cdot \mathbf{v}_g)^2 = \frac{\omega_{pe}^2 k^4 R^4}{4} \left[1 - \frac{|E_0|^2}{8\pi n_0 M R^2 \Omega_k^2} \right], \quad (38)$$

where \mathbf{v}_g is the group velocity of the UH wave. Equation (38) predicts the instability when $|E_0|^2 > 8\pi n_0 M R^2 \Omega_k^2$. In the opposite case of long-wavelength pump $\mathbf{k} \gg \mathbf{k}_0$ Eq. (36) is reduced to

$$\Omega^2 = \frac{1}{2} \left\{ \delta^2 + \Omega_k^2 \pm \sqrt{(\delta^2 - \Omega_k^2)^2 + \frac{|E_0|^2 \omega_{pe} k^2 \delta}{4\pi n_0 M}} \right\}, \quad (39)$$

where $\delta = \omega_{UH} k^2 R^2 / 2$ and, thus, there is a purely growing instability for sufficiently large amplitudes of the pump wave E_0 .

IV. PROOF OF ABSENCE OF COLLAPSE

In what follows, we will consider the case $\omega_{ce}^2/\omega_{pe}^2 \ll 1$, so that vector nonlinearities in Eqs. (6) and (22) can be neglected. Then, introducing the dimensionless variables

$$t \rightarrow \omega_{LH} t, \quad \mathbf{r} \rightarrow \mathbf{r} \omega_{LH} / v_s, \quad (40)$$

$$\varphi \rightarrow \varphi \frac{\omega_{pi}}{4v_s \sqrt{\pi n_0 T_e}}, \quad b \rightarrow \frac{\delta B}{B_0} \frac{\omega_{pe}^2}{\omega_{ce}^2 \beta}, \quad (41)$$

$$\mu = \frac{2\omega_{UH} m}{3\omega_{LH} M}, \quad \beta = \frac{v_s^2}{v_A^2}, \quad (42)$$

and eliminating $\delta n/n_0$, one can rewrite Eqs. (6), (22) and (23) as follows

$$\Delta \left(i\mu \frac{\partial \varphi}{\partial t} + \Delta \varphi \right) = \nabla \cdot [(\beta b - \Delta b) \nabla \varphi], \quad (43)$$

$$\left(\frac{\partial^2}{\partial t^2} - \Delta \right) (\beta - \Delta) b - \Delta b = \Delta |\nabla \varphi|^2, \quad (44)$$

Equations (43) and (44) conserves energy

$$N = \int |\nabla \varphi|^2 d\mathbf{r}, \quad (45)$$

and Hamiltonian

$$H = \int \left(|\Delta \varphi|^2 + \frac{1}{2} |\nabla \varphi|^2 (\beta - \Delta) b \right) d\mathbf{r}, \quad (46)$$

and can be written in the Hamiltonian form

$$-i\mu \Delta \frac{\partial \varphi}{\partial t} = \frac{\delta H}{\delta \varphi^*}. \quad (47)$$

In this section, following the ideas suggested in Ref. 14, we present a rigorous proof of the absence of collapse for the stationary 2D solutions of the form $\varphi(x, y, t) = \psi(x, y) \exp(i\Lambda t)$ in the model described by Eqs. (43) and (44). We use an exact approach¹⁶ based on the Liapunov stability theory. Let us briefly recall the essence of the Liapunov method. For an invariant set of the dynamical system (in particular, for the set of stationary solutions $\{u_s\}$) to be stable, it is sufficient that there exists a functional $L[u]$ with the following properties: a) L is the positive definite functional for the perturbed states $\{u\}$, i.e. $L[u] \geq 0$; b) L reaches its minimum on the set $\{u_s\}$, $L[u_s] = 0$; c) L is nonincreasing function of time t , i.e. $dL/dt \leq 0$. For hamiltonian systems, these conditions are equivalent to the requirement that the Hamiltonian is bounded from below under the fixed conserved quantity N (then, one can choose $L = H - H_{min}$). Then, the 2D stationary localized solutions corresponding to the global minimum of H (fundamental solitons) are stable in the Liapunov sense.

Note, that for the stationary solutions, Eqs. (43) and (44) can be rewritten as follows

$$\Delta(-\Lambda \mu + \Delta) \psi = \nabla \cdot [(\beta - \Delta) b \nabla \psi], \quad (48)$$

with

$$b(\mathbf{r}) = - \int G(\mathbf{r} - \mathbf{r}') |\nabla \varphi(\mathbf{r}')|^2 d\mathbf{r}', \quad (49)$$

where $G(\mathbf{r}) = K_0(\sqrt{\beta+1}|\mathbf{r}|)/2\pi$ is the Green function satisfying the equation $(\beta+1-\Delta)G(\mathbf{r}) = \delta(\mathbf{r})$, and $K_0(z)$ is the modified Bessel function of the second kind of order zero. It is seen, that the nonlinearity in Eq. (48) has essentially nonlocal character. We represent the Hamiltonian (46) as

$$H = A + \frac{1}{2} P, \quad (50)$$

where $A = \int |\Delta \psi|^2 d\mathbf{r}$ and the nonlinear term P can be written as

$$\begin{aligned} P &= - \int |\nabla \varphi(\mathbf{r})|^2 |\nabla \varphi(\mathbf{r}')|^2 (\beta - \Delta) G(|\mathbf{r} - \mathbf{r}'|) d\mathbf{r} d\mathbf{r}' \\ &= - \int |\nabla \varphi(\mathbf{r})|^4 d\mathbf{r} + C, \end{aligned} \quad (51)$$

where

$$C = \int |\nabla\varphi(\mathbf{r})|^2 |\nabla\varphi(\mathbf{r}')|^2 G(|\mathbf{r} - \mathbf{r}'|) d\mathbf{r} d\mathbf{r}' > 0. \quad (52)$$

To get an estimate for C we use the following inequality¹⁴

$$\int \frac{f^2(\mathbf{r})}{|\mathbf{r} - \mathbf{r}'|} d\mathbf{r} \leq 2 \left(\int f^2 d\mathbf{r} \right)^{1/2} \left(\int (\nabla f)^2 d\mathbf{r} \right)^{1/2}, \quad (53)$$

where $f(\mathbf{r})$ is an arbitrary sufficiently smooth function, the integration in Eq. (53) is performed over entire 2D space. We have

$$\begin{aligned} C &= \int |\nabla\varphi(\mathbf{r})|^2 \frac{|\nabla\varphi(\mathbf{r}')|^2}{|\mathbf{r} - \mathbf{r}'|} G(|\mathbf{r} - \mathbf{r}'|) |\mathbf{r} - \mathbf{r}'| d\mathbf{r} d\mathbf{r}' \\ &\leq M \int |\nabla\varphi(\mathbf{r})|^2 d\mathbf{r} \int \frac{|\nabla\varphi(\mathbf{r}')|^2}{|\mathbf{r} - \mathbf{r}'|} d\mathbf{r}' \\ &\leq 2M \left(\int |\nabla\varphi(\mathbf{r})|^2 d\mathbf{r} \right)^{3/2} \left(\int |\Delta\varphi(\mathbf{r})|^2 d\mathbf{r} \right)^{1/2} \\ &= 2MN^{3/2}A^{1/2}, \end{aligned} \quad (54)$$

where $M = \max_z [zK_0(z\sqrt{\beta+1})/2\pi] > 0$ and we have used Eq. (53). Next we use the inequality

$$\int |\nabla\varphi(\mathbf{r})|^4 d\mathbf{r} \leq N^2. \quad (55)$$

As a result, one can write the obvious chain of inequalities:

$$P \geq -N^2 + C \geq -N^2 - C \geq -N^2 - 2MN^{3/2}A^{1/2}. \quad (56)$$

Inserting this estimate into the expression for the hamiltonian Eq. (50) we get

$$H \geq A - \frac{1}{2}N^2 - MN^{3/2}A^{1/2}. \quad (57)$$

Under the fixed N , the right hand side of the inequality (57) reaches its minimum at $A = M^2N^3/4$, so that

$$H \geq -M^2N^3/4 - N^2/2. \quad (58)$$

Thus, we have showed that, under the fixed conserved quantity N , the Hamiltonian is bounded from below. According to standard Liapunov theory, this represents a rigorous proof that a collapse with the wave amplitude locally going to infinity cannot occur for the stationary solutions in the model described by Eqs. (43) and (44).

V. NONLINEAR LOCALIZED SOLUTIONS

We consider the case when the upper-hybrid wavelength is much smaller than the typical spatial scale of the localization and represent (in the corresponding dimensionless variables)

$$\varphi = \Phi \exp(i\mathbf{k}_0 \cdot \mathbf{r} - i\delta_0 t). \quad (59)$$

We assume that $k_0L \gg 1$, where $L = |\psi/\nabla\psi|$ is the typical length scale of the low-frequency perturbation. We also make an additional assumption of $\mathbf{k}_0 \cdot \nabla = 0$. Under this, the group velocity of the upper-hybrid wave is perpendicular to the direction of inhomogeneity and there is no transportation of energy in the direction of inhomogeneity which results in stationary envelope structure in the direction perpendicular to the magnetic field. Then, the system Eqs. (43) and (44) takes the form

$$i\mu \frac{\partial \Phi}{\partial t} + \Delta \Phi = (\beta - \Delta)b\Phi, \quad (60)$$

$$\left(\frac{\partial^2}{\partial t^2} - \Delta \right) (\beta - \Delta)b - \Delta b = \Delta|\Phi|^2, \quad (61)$$

where we have rescaled Φ so that $\Phi \rightarrow k_0\Phi$. The proof of the absence of collapse for the stationary solutions of the system (60) and (61) is quite analogous to that presented in the previous section.

We look for stationary solutions of Eqs. (60) and (61) in the form $\Phi(x, y, t) = \Psi(x, y) \exp(i\lambda t/\mu)$, where λ/μ is the nonlinear frequency shift, so that Ψ obeys the equation

$$-\lambda\Psi + \Delta\Psi = (\beta - \Delta)b\Psi, \quad (62)$$

$$(\beta + 1 - \Delta)b = -|\Psi|^2. \quad (63)$$

To solve numerically Eqs. (62) and (63), we impose periodic boundary conditions on Cartesian grid and use the relaxation technique similar to one described in Ref. 17. Choosing an appropriate initial guess, one can find numerically with high accuracy (the norms of the residuals were less than 10^{-9}) three different classes of spatially localized solutions of Eqs. (62) and (63) – the nonrotating (multi)solitons, the radially symmetric vortices, and the rotating multisolitons (azimuthons).

The real (or containing only a constant complex factor) function $\Psi(x, y)$ corresponds to nonrotating solitary structures. Examples of such nonrotating (multi)solitons for Eqs. (62) and (63), namely, a monopole, a dipole, two-hump soliton, and a quadrupole are presented in Figs. 1(a)- 1(d) for the case $\beta = 0.1$. The analogous solutions can be found for $\beta > 1$. The nonrotating multipoles consist of several fundamental solitons (monopoles) with opposite phases.

The second class of solutions, vortex solutions, are the solutions with the radially symmetric amplitude $|\Psi(x, y)|$, that vanishes at the center, and a rotating spiral phase in the form of a linear function of the polar angle θ , i.e. $\arg \Psi = m\theta$, where m is an integer. The index m (topological charge) stands for a phase twist around the intensity ring. The important integral of motion associated with this type of solitary wave is the z -component of the angular momentum

$$M_z = \text{Im} \int [\Phi^*(\mathbf{r} \times \nabla_\perp \Phi)]_z d\mathbf{r}, \quad (64)$$

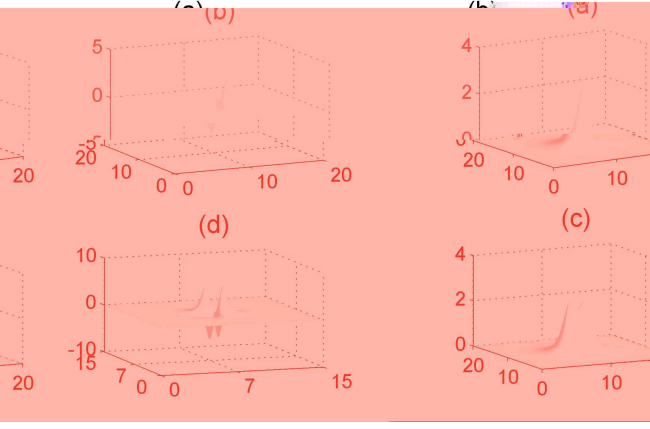


FIG. 1: Numerically found nonrotating stationary localized solutions of Eqs. (60) and (61) for $\beta = 0.1$: (a) monopole with $\lambda = 0.5$; (b) dipole with $\lambda = 0.5$; (c) two-hump soliton with $\lambda = 0.5$; (d) quadrupole with $\lambda = 2$. The real part of the field Ψ is shown.

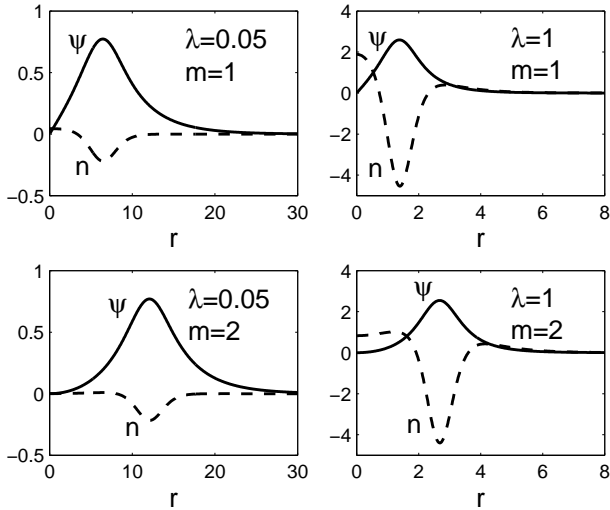


FIG. 2: Examples of the stationary radially symmetric vortex solutions, characterized by the topological charges $m = 1, 2$ for $\lambda = 0.05$ (left panel) and $\lambda = 1$ (right panel): radial profiles of the field intensity $|\Psi|$ (solid curve) and density n (dashed curve) are shown for $\beta = 0.25$.

which can be expressed through the soliton amplitude U and phase ϕ ,

$$M_z = \int \frac{\partial \phi}{\partial \theta} U^2 d\mathbf{r}, \quad (65)$$

and for the vortex we have $M_z = mN$. Examples of the stationary radially symmetric vortex solutions, characterized by the topological charges $m = 1, 2$ for different values of λ are shown in Fig. 2.

The third class of solutions, rotating multisolitons with the spatially modulated phase, were first introduced in Ref. 18 for models with local nonlinearity, where they

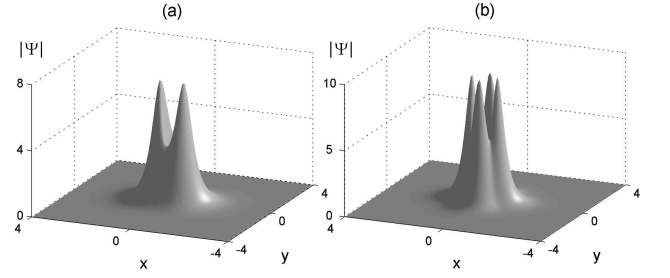


FIG. 3: Examples of the rotating multisolitons (azimuthons) with $\lambda = 5$ for $\beta = 0.1$: a) azimuthon with two intensity peaks; b) azimuthon with four intensity peaks. The field intensity $|\Psi|$ is shown.

were called azimuthons. The azimuthons can be viewed as an intermediate kind of solutions between the rotating radially symmetric vortices and nonrotating multisolitons. Using variational analysis to describe azimuthons, the authors of Ref. 12 considered the following trial function in polar coordinates (r, θ)

$$\Psi(r, \theta) = r^{|m|} \Phi(r) (\cos m\theta + ip \sin m\theta), \quad (66)$$

where Φ is the real function, which vanish fast enough at infinity, m is an integer, and $0 \leq p \leq 1$. The case $p = 0$ corresponds to the nonrotating multisolitons (e. g. $m = 1$ to a dipole, $m = 2$ to a quadrupole etc.), while the opposite case $p = 1$ corresponds to the radially symmetric vortices. The intermediate case $0 < p < 1$ corresponds to the azimuthons. The trial function Eq. (66) was chosen as an initial guess in our numerical relaxation method. Then, the numerically found complex function $\Psi(x, y)$ with a spatially modulated phase corresponds to the azimuthons. We introduced the parameter p (modulational depth), which is similar to the one in Eq. (66), in the following way

$$p = \max |\text{Im } \Psi| / \max |\text{Re } \Psi|. \quad (67)$$

For fixed λ , there is a family of azimuthons with different p . Since the azimuthons have a nontrivial phase, they, like the radially symmetric vortices, carry out the nonzero angular momentum. In Figures 3 we demonstrate two numerically found examples of the azimuthons with two and four intensity peaks for the nonlocal model described by Eqs. (62) and (63). The azimuthon with two intensity peaks consists of two dipole-shaped structures in the real and imaginary parts of Ψ with different amplitudes and the ratio of these amplitudes is the modulational depth p . Note, that the choice of initial guess in the relaxation method for finding the azimuthons is much more sophisticated than that for the nonrotating multisolitons or vortices. For example, we were not able to find azimuthon solutions with predetermined (in advance) value of p .

We next addressed the stability of these localized solutions and study the evolution of the solitons in the presence of small initial perturbations. We have undertaken

extensive numerical modeling of Eqs. (60) and (61) initialized with our computed solutions with added gaussian noise. The initial condition was taken in the form $\Psi(x, y)[1 + \varepsilon f(x, y)]$, where $\Psi(x, y)$ is the numerically calculated exact solution, $f(x, y)$ is the white gaussian noise with variance $\sigma^2 = 1$ and the parameter of perturbation $\varepsilon = 0.005 \div 0.01$. In addition, azimuthal perturbation of the form $i\varepsilon \sin \theta$ was taken for the vortices and azimuthons. Spatial discretization was based on the pseudospectral method. Temporal t -discretization included the split-step scheme.

Numerical simulations clearly show that the fundamental solitons are stable and do not collapse even for the negative initial hamiltonian. Stable evolution of the monopole soliton with $\lambda = 1$ is shown in Fig. 4(a). We have observed neither stable evolution nor collapse for multisolitons. If the nonlinear frequency shift λ is not too large, the multisolitons decay into several monopole solitons, but can survive over quite considerable times. Splitting of the dipole soliton in two monopoles which move in the opposite directions without changing their shape is shown in Fig. 4(b). Figure 5 presents an example of the decay of the vortex into three fundamental solitons. Since the total angular momentum is conserved, the monopole solitons fly off the ring along tangential trajectories. A similar behavior was observed for the rotating multisolitons (azimuthons with two and four intensity peaks). If the nonlinear frequency shift λ exceeds some critical value depending on the multisoliton type (i.e. dipole, azimuthon with two intensity peaks etc.), the unstable multisoliton turn into the one monopole with larger amplitude. Although the multisolitons turn out to be unstable in all our runs, one cannot exclude the possibility of existence of stable multisolitons in some narrow range of parameters (see, for example, Refs. 19 and 20). A rigorous proof of the stability/instability could give a linear stability analysis with the corresponding eigenvalue problem.

Soliton structures can arise as the result of modulational instability of the initial monochromatic UH pump wave. We numerically studied the evolution of a monochromatic long wavelength UH wave in the framework of Eqs. (60) and (61). Consider the case when a monochromatic UH wave of the form

$$\Phi(x, y) = 1.5 \exp(0.07ix + 0.07iy) \quad (68)$$

is chosen as an initial condition in a box of side $L = 10$. Thus, the wave Eq. (68) represents the almost homogeneous initial field. The time evolution of the field Eq. (68) is shown in Fig. 6. It is clearly seen the formation of one well-shaped soliton, which moves in some direction with almost no change in shape and at later times coexists with turbulent environment. Depending on the amplitude and wave vector of the pump as well as on the box length, we observed the formation of two and more solitons, and even, in some cases, the formation (simultaneously with solitons) of structures resembling the ring-like vortices. No soliton formation, however, was

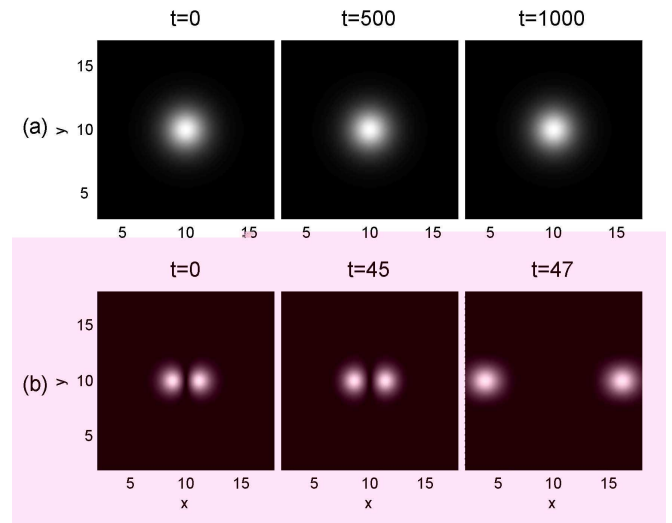


FIG. 4: (a) Stable evolution of the monopole with $\lambda = 1$; (b) splitting of the dipole with $\lambda = 2$ into two monopoles.

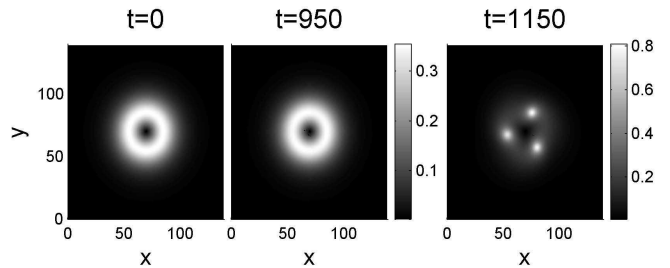


FIG. 5: Evolution of the vortex with $m = 1$ and $\lambda = 0.01$ for $\beta = 0.25$.

detected in all cases if the amplitude of the initial pump was sufficiently small (for example, less than 0.8 for Eq. (68)) so that, for a given grid, box size and the wave vector of the pump, the threshold of the modulational instability was not exceeded. It is important, that in all our numerical simulations of the evolution of initial fields we did not observed any evidence of collapse.

VI. CONCLUSION

In the present paper, we have considered the nonlinear interaction between dispersive magnetosonic and high-frequency UH waves ion 2D geometry. We have derived a set of 2D equations describing the dynamics of nonlinearly coupled magnetosonic and UH waves. Nonlocal nonlinearity in the equations prevents collapse and results in the possibility of existence of stable 2D nonlinear structures. We have presented a rigorous proof of the absence of collapse in the model under consideration. We have found numerically different types of nonlinear 2D localized structures such as fundamental solitons, radially symmetric vortices, nonrotating multi-

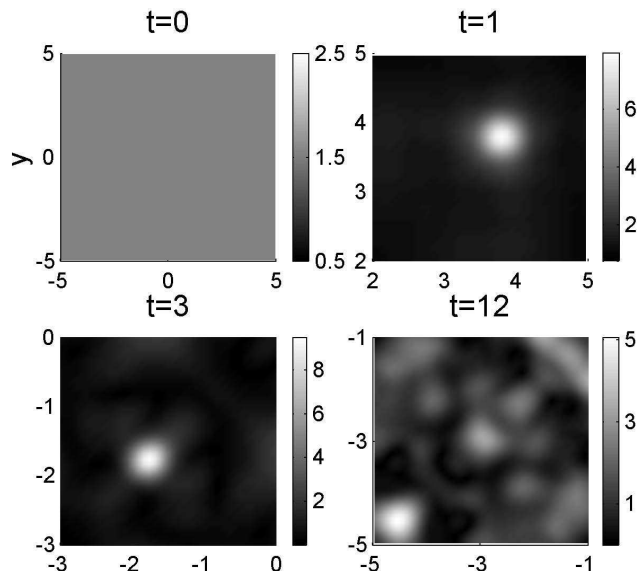


FIG. 6: Evolution of the almost homogeneous initial field Eq. (68) in the model Eqs. (60) and (61). The panels show the intensity $|\Phi|$ in the (x, y) plane at times $t = 0$, $t = 1$, $t = 3$, and $t = 12$, respectively. The modulational instability of the initial field results in emergence of a self-localized state (soliton).

solitons (dipoles and quadrupoles), and rotating multi-solitons (azimuthons). By direct numerical simulations we have shown that fundamental solitons are stable and do not collapse even with negative initial hamiltonian. Multisolitons and vortices decay into fundamental solitons but can survive over quite considerable times.

-
- * Electronic address: vlashkin@kinr.kiev.ua
- ¹ P. K. Shukla, R. Fedele, and U. de Angelis, Phys. Rev. A **31**, 517 (1985).
 - ² A. N. Kaufman and L. Stenflo, Phys. Scripta **11**, 269 (1975).
 - ³ M. Porkolab and M. V. Goldman, Phys. Fluids **19**, 872 (1976).
 - ⁴ I. A. Kolchugina, A. G. Litvak and A. M. Sergeev, JETP Lett. **35**, 631 (1982).
 - ⁵ A. G. Litvak, V. I. Petrukhina, A. M. Sergeev and G. M. Zhislin, Phys. Lett. A **94**, 85 (1983).
 - ⁶ R. P. Sharma and P. K. Shukla, Phys. Fluids **26**, 87 (1983).
 - ⁷ B. Eliasson and P. K. Shukla, Phys. Plasmas **10**, 3539 (2003).
 - ⁸ A. I. Yakimenko, Yu. A. Zaliznyak, and Yu. Kivshar Phys. Rev. E **71**, 065603 (2005).
 - ⁹ D. Briedis, D. E. Petersen, D. Edmundson, W. Krolikowski, and O. Bang, Opt. Express **13**, 435 (2005).
 - ¹⁰ A. I. Yakimenko, V. M. Lashkin, and O. O. Prihodko, Phys. Rev. E **73**, 066605 (2006).
 - ¹¹ Y.V. Kartashov, L. Torner, V. A. Vysloukh, and D. Mihalache, Opt. Lett. **31**, 1483 (2006).
 - ¹² S. Lopez-Aguayo *et al.*, Opt. Lett. **31**, 1100 (2006).
 - ¹³ S. Skupin, O. Bang, D. Edmundson, and W. Krolikowski, Phys. Rev. E **73**, 066603 (2006).
 - ¹⁴ S. K. Turitsyn, Teor. Mat. Fiz. **64**, 226 (1985) [Theor. Math. Phys. **64**, 797 (1985)].
 - ¹⁵ W. Krolikowski, O. Bang, N. I. Nikolov, D. Neshev, J. Wyller, J. J. Rasmussen, and D. Edmundson, J. Opt. B **6**, S288 (2004).
 - ¹⁶ V. E. Zakharov and E. A. Kuznetsov, Zh. Eksp. Teor. Fiz. **66**, 594 (1974) [Sov. Phys. JETP **39**, 285 (1974)].
 - ¹⁷ V.I. Petviashvili and V.V. Yan'kov, in *Reviews of Plasma Physics*, edited by B. B. Kadomtsev, (Consultants Bureau, New York, 1989), Vol. 14.
 - ¹⁸ A. S. Desyatnikov, A. A. Sukhorukov, and Yu. S. Kivshar, Phys. Rev. Lett. **95**, 203904 (2005).
 - ¹⁹ V. M. Lashkin, Phys. Rev. A **75**, 043607 (2007).
 - ²⁰ V. M. Lashkin, A. I. Yakimenko, and O. O. Prihodko, Phys. Lett. A **366**, 422 (2007).